Measured atomic ground-state polarizabilities of 35 metallic elements

Lei Ma, John Indergaard, Baiqian Zhang, Ilia Larkin, Ramiro Moro, and Walt A. de Heer

Phys. Rev. A **91**, 010501 — Published 7 January 2015

DOI: 10.1103/PhysRevA.91.010501

Measured atomic ground state polarizabilities of 35 metallic elements.

[1]Lei Ma [1]John Indergaard [1]Baiqian Zhang [1]Ilia Larkin [2]Ramiro Moro [1]*Walt A. de Heer

[1] School of Physics, Georgia Institute of Technology, Atlanta, GA 30332
[2]Cameron University, Lawton, OK 73505

Abstract: Advanced pulsed cryogenic molecular beam electric deflection methods involving position-sensitive mass spectrometry and 7.87 eV ionizing radiation were used to measure the polarizabilities of more than half of the metallic elements in the periodic table for the first time. Concurrent Stern-Gerlach deflection measurements verified the ground state condition of the measured atoms. Comparison with state-of-the-art calculations exposes significant systematic and isolated discrepancies throughout the periodic table.

Keywords: Static polarizability, molecular beam, position-sensitive time-of-flight mass spectrometry

The static dipole polarizability is a fundamental ground state property of atoms that has been measured for a few atoms with high precision, for example [1-3]. Despite its relevance, the polarizabilities of less than 1/4 of the elements in the periodic table have ever been measured. Not only are atomic polarizabilities important for a variety of applications [4-12], but they also continue to serve as tests for many-body computational methods, which are particularly challenging for atoms with many valence electrons. However, due to the lack of experimental data often comparisons can only be made with other calculations [13-17]. Here we present the polarizabilities of Na*, Mg, Al*, Sc, Ti, V, Cr, Cu, Ga, Y, Zr, Nb, Mo, Rh, Ag, In*, Sn*, La, Ce, Pr, Nd, Sm, Eu, Gd, Tb, Dy, Ho, Er, Tm, Yb, Lu, Hf, Ta, Pb*, and Bi (* indicates prior measurement). We show that even when distinct theoretical methods mutually agree [18], surprisingly, in some cases, they disagree with experiment by more than

30%. Rhodium is an extreme case, where the measured polarizability is at least a factor of 2 smaller than the calculated one.

Earlier measurements relied on techniques that required intense and stable molecular beams. For example, in the E-H balance method the beam passes through an inhomogeneous electric field and an inhomogeneous magnetic field. The fields are adjusted so that the deflections compensate to provide a relationship between the magnetic and induced electric dipole moment [19, 20]. The method does not require a measurement of the speed of the atoms, but it does require ground state paramagnetic atoms with known magnetic moments. Polarizability measurements using the interference of two atomic beams originating from a single source [3, 21] are accurate (better than 1%) but the method is not universally applicable.

Metal atoms are particularly challenging, since most have several very low-lying excited states that are typically excited when using standard molecular beam methods. (For example, Al has an excited state at 112 cm^{-1}, V at 137 cm^{-1}, Nb at 154 cm^{-1}, Sc at 168 cm^{-1}, Ti at 170 cm^{-1}, Gd at 215 cm^{-1}, Ce at 229 cm^{-1}, etc. [22]) Consequently, the measurements will not reliably reflect the ground state polarizabilities. These challenges explain why the atomic polarizabilities of so few elements, and metals in particular, have been measured [18, 23].

The molecular beam apparatus used in the measurements presented here overcomes the experimental obstacles above, allowing accurate polarizability

measurements to be performed on the ground state of any stable atom. In principle, this method requires neither intense nor stable beams. The technique is limited essentially only by the photon energy of the laser used to ionize the atoms, as explained next.

The apparatus is schematically shown in Fig. 1. Briefly (for details Ref. [24]), atoms are produced in a laser vaporization source where pulsed light from a Nd:YAG laser (532 nm, 8 ns pulse width, less than 4 mJ/pulse, 10 Hz) is focused on a metal target in the cryogenically cooled source (whose temperature can be adjusted from T=10 K to 300 K), vaporizing a minute amount of metal, on the order of 10^{-3} cm^3/hour (the target rods were produced from metals obtained from Alfa Aesar with a purity of 99.95% or better). The metal vapor cloud is entrained in a pulse of cryogenically cooled He injected in the source, that cools the vapor, to produce a mixture of atoms and clusters that emerge from a 0.5 mm diameter nozzle. The source parameters are optimized for each material. The resulting beam is collimated using a series of slits and negotiates an inhomogeneous electric field produced by electrodes in the standard "two-wire field" geometry [25, Supp. Mat.], that is activated to a voltage V≤20 kV, to produce electric fields E≤85 kV/cm, dE/dz≤218 kV/cm^2. The deflected beam ultimately enters the position-sensitive time-of-flight mass spectrometer (PSTOF), where a pulse of ionizing radiation supplied by an F_2 excimer laser (157 nm, 7.89 eV) ionizes a fraction of the atoms (and clusters, when present). A pulsed electric field accelerates the ions towards the ion detector and the arrival time of the ions are digitally recorded using a multichannel scalar with 500 ps

channel bin widths. The electric fields in the TOF are adjusted so that the resulting peaks in the TOF spectrum reveal the position of all of the ions in the beam at the time of ionization (see Fig. 2(a, b)). When the deflection field is activated, the deflections are manifested as an essentially rigid shift of the beam (with respect to the field-off condition) by a distance *d* in the direction of the deflecting electric field gradient. This shift is accurately measured by interleaving field-on and field-off measurements (Fig. 2(a, b)). Standard data analysis allows the deflections to be evaluated with a typical accuracy of 10 μm. This accuracy is ultimately determined only by counting statistics, and not by the beam width, nor beam stability, nor the temporal separation of the channels in the multichannel scalar. (For details of the data analysis, see Ref. [26-29].) When the TOF fields are adjusted for the high-resolution mass spectrometry mode, the peaks do not shift, and the TOF has a mass resolution $m/\Delta m=10^4$ (in the position-sensitive mode $m/\Delta m=10^3$), as shown in Fig. 2(a, b). The parameters in the TOF can be instantaneously switched from position insensitive high-resolution mass spectroscopy mode (also known as spatial focusing mode) to the position-sensitive mass spectroscopy mode. This flexibility allows us to simultaneously measure the electric deflections of elements with several isotopes, as shown in Fig. 2(g) in the case of Sn.

A chopper just down-stream of the source passes a small pulse of atoms in each cycle (for details, see Ref. [24, 30]). The ionization laser is synchronized with the chopper. The velocity of the selected atoms is evaluated with typically 0.5% accuracy. The polarizability α is found from

$$d = \alpha E \frac{\partial E}{\partial z}\left(L + \frac{l}{2}\right)\frac{l}{mv^2} = K\alpha\frac{V^2}{mv^2} \qquad \text{(Eq. 1)}$$

where E is the electric field (proportional to the applied voltage V), $\partial E/\partial z$ is the field gradient in the inhomogeneous electric field, L is the distance from the field to the detector and l is the length of the deflecting field. K lumps these constants together. Since Al reliably produces intense atomic beams we used Al as our standard reference. Calibration runs using Al were performed in the course of each measurement. The quality of Al calibration (measured to be α_{Al}=6.8±0.3 Å^3 in [24]) can be judged based on the comparison between our measured value of α_{Na}=23.8±1.1 Å^3 for sodium and ultra-high precision measurement made in Ref. [3]). Note that the same apparatus was used for metal cluster polarizability measurements [31, 32], for which the polarizabilities are found to accurately converge to their bulk metal limits (i.e. $\alpha_{bulk}=R^3_{bulk}$, where R_{bulk} is the bulk atomic radius [33]).

The molecular beam apparatus is also supplied with a Stern-Gerlach magnet (see Fig. 1). The number of peaks in the magnetic deflections (see Fig. 2(c-f)) of a specific atom corresponds to 2J+1, where J is the atomic angular momentum quantum number, whose value is known for all ground states and excited states of the atoms measured. We have verified that the atoms were indeed in their ground states (note that we were also able to produce beams at higher temperatures that contained excited state atoms (Fig. 2(e, f)), but no attempts were made to measure excited state polarizabilities). The atomic beam temperature is determined from the relative

population of the excited states to ground states using Boltzmann statistics, revealing that it closely follows the source temperature [Supp. Mat]. This indicates that the source effectively cools the atoms. It is particularly important for atoms which have excited states that are excited even below room temperature (i.e. Al, Sc, Ti, V, and Nb), requiring the efficient cryogenic cooling provided by our source.

Results of the measurements are reported in Table 1 and plotted in Fig. 3 that also presents theoretical results. The well-known shell structure trend, where the polarizability is the greatest at the opening of an atomic shell (i.e. at the alkalis) and progressively diminishes at the closing of the shell (i.e. at the inert gasses) is clearly observed. Our measurements agree with measurements of 5 elements (Na, Al, In, Sn and Pb) that were previously measured. However significant discrepancies are observed for theoretical predictions of specific atoms as well as in trends. For example, α_{Al} is measured to be 20% smaller than several calculations, and α_{Mg} is also smaller than the predicted value. For the 4d transition metals, the local density approximation (LDA) predictions agree with the experimental values, but it significantly overestimates the polarizabilities for the 3d and 5d metals. The variational perturbation approach (VPA) appears to be more accurate for the 3d metals, but still large discrepancies (>30% for Ti) are observed [18]. For Cu, experiment and theory agree well. On the other hand, $_{45}$Rh ($4d^8\,5s^1$) the measured polarizability is 1.6 Å^3 (comparable to $_{36}$Kr), while the predicted value is 8.57 Å^3, representing the largest discrepancy that we have measured. The LDA predictions for the lanthanides (4f) are reasonably accurate, however non-systematic

discrepancies (both positive and negative) on the order of 20% are observed. Polarizabilities of the p-block metals (Fig. 3(d)) show significant discrepancies for Al and Ga, but In, Sn, Pb and Bi are all in reasonable agreement with various theories.

In conclusion, despite their importance for atomic physics and computational physics, atomic polarizabilities of relatively few atoms had been measured prior to this work. Here we have presented the ground state polarizabilities of half of the (stable) metallic elements in the periodic table. Experiment and theory agree well in about half of the cases. Several significant systematic discrepancies (e.g. in the 3d metals) and several isolated large discrepancies (i.e. Al and Rh) compared with theory were noted. Since various theoretical approaches tend to agree with each other better than with experiment, it suggests that our measurements may have uncovered systematic theoretical problems and therefore may help future developments in many-body theory. The accuracy of the measurements provided here can be significantly improved with further developments of the technique. These polarizability measurements will be extended to dimers, many of which have been calculated, but not measured.

Acknowledgements

The National Science Foundation is gratefully acknowledged for financial support under grant DMR1308835

Table 1. A comprehensive table containing atomic number, electronic configuration, term symbol, as well as our measured polarizabilities and uncertainties for each element studied in this work. Uncertainty shown here do not include the contribution from the Al calibration. (*the polarizability for Rh is anomalously low)

FIG. 1. Cryogenic molecular beam apparatus with position-sensitive time-of-flight mass spectrometer for electric and magnetic deflection measurements. To scale; source to TOF distance is 2.5 m. 1: YAG laser (Continuum, Surelite I-20, 2nd and 3rd harmonic); 2: Lens; 3: Window; 4: Cryogenic laser vaporization source with cryogenic pulsed valve; 5: Skimmer; 6: He carried beam; 7: Cryogenic system (Sumitomo SRDK); 8: Pre-collimator; 9: Collimators with micrometer activation; 10: Ultrafast high voltage switch (Behlke HTS31); 11: MgF_2 window; 12: F_2 Excimer laser (GAM EX5).

FIG. 2 Examples of atomic beam time-of-flight profiles of several elements; raw data presented as counts in the indicated time channel (channel 0 is defined to correspond to beam center of the field off peak for (a)-(f)). Fits are shown as continuous lines. In (a) and (b) high-resolution (HR, position insensitive) peaks are shown in blue (dashed grey line), while position-sensitive with field off is shown in green (grey line), and with field on is shown in red (black line). (a) Electric deflections of ground state Al, source temperature T=20 K; (b) Electric deflections of Nb at T=20 K; (c) Stern-Gerlach deflections of Al at T=20 K correspond to the $^2P_{1/2}$ ground state; (d) Stern-Gerlach deflections of Al at T=295 K; an admixture of the $^2P_{3/2}$ excited state (E=112 cm^{-1}) is observed; (e) Stern-Gerlach deflections of Nb at T=20 K showing the $^6D_{1/2}$ ground state, and (f) at T=295 K revealing an admixture of

$^6D_{3/2}$ (E=154 cm^{-1}); (g) PSTOF of Sn, showing the electric deflections of 8 of its stable isotopes indicated by their atomic masses (in atomic units); spurious additional peaks are from the residual gas in the detector.

FIG. 3 Overview of atomic polarizabilities. (a-f) Measured and calculated polarizabilities organized by atomic orbital type, s, p, d, and f. (g) Calculated values (open blue circles, from Ref. 18 and references therein); Previously measured values (green squares, from Ref. [3, 21, 27, 34]); Measured values in this work (red triangles).

Element		Config.	Term	Pol.(Å^3)	Unc.(Å^3)		Element		Config.	Term	Pol.(Å^3)	Unc.(Å^3)
11	Na	$3s^1$	$^2S_{1/2}$	23.8	1.1		58	Ce	$4f^15d^16s^2$	$^1G°_4$	28.4	3.0
12	Mg	$3s^2$	$^1S_0$	8.8	2.3		59	Pr	$4f^36s^2$	$^4I°$	35.4	4.1
13	Al	$3s^24s^1$	$^2P°_{1/2}$	6.8	0.3		60	Nd	$4f^46s^2$	$^5I_4$	27.2	2.9
21	Sc	$3d^14s^2$	$^2D_{3/2}$	14.4	1.4		62	Sm	$4f^66s^2$	$^7F_0$	23.2	2.4
22	Ti	$3d^24s^2$	a $^3F_2$	9.4	0.5		63	Eu	$4f^76s^2$	a $^8S°_{7/2}$	21.6	3.7
23	V	$3d^34s^2$	a $^4F_{3/2}$	10.1	0.8		64	Gd	$4f^75d^16s^2$	$^9D°_2$	26.1	3.9
24	Cr	$3d^54s^1$	a $^7S_3$	8.9	3.5		65	Tb	$4f^96s^2$	$^6H°_{15/2}$	23.5	1.6
29	Cu	$3d^{10}4s^1$	$^2S_{1/2}$	8.7	0.7		66	Dy	$4f^{10}6s^2$	$^5I_8$	23.3	1.6
31	Ga	$4s^24p^1$	$^2P°_{1/2}$	6.9	0.6		67	Ho	$4f^{11}6s^2$	$^4I°_{15/2}$	21.5	1.7
39	Y	$4d^15s^2$	$^2D_{3/2}$	24.1	1.7		68	Er	$4f^{12}6s^2$	$^3H_6$	32.2	5.7
40	Zr	$4d^25s^2$	a $^3F_2$	16.6	1.9		69	Tm	$4f^{13}6s^2$	$^2F°_{7/2}$	19.2	2.4
41	Nb	$4d^45s^1$	a $^6D_{1/2}$	14.5	1.1		70	Yb	$4f^{14}6s^2$	$^1S_0$	21.8	2.9
42	Mo	$4d^55s^1$	a $^7S_3$	12.9	0.9		71	Lu	$5d^16s^2$	$^2D_{3/2}$	18.3	2.7
45	Rh	$4d^85s^1$	a $^4F_{9/2}$	1.6*	-1.6/+3.2*		72	Hf	$5d^26s^2$	$^3F_2$	12.4	2.8
47	Ag	$4d^{10}5s^1$	$^2S_{1/2}$	6.8	1.1		73	Ta	$5d^36s^2$	$^4F_{3/2}$	8.6	1.8
49	In	$5p^1$	$^2P°_{1/2}$	9.2	0.9		82	Pb	$6p^2{}_{1/2}$	$(^1/_2,^1/_2)$	8.3	2.7
50	Sn	$5p^2$	$^3P_0$	10.0	1.3		83	Bi	$6p^3$	$^4S°_{3/2}$	8.1	1.7
57	La	$5d^16s^2$	$^2D_{3/2}$	25.3	1.2							

Table 1

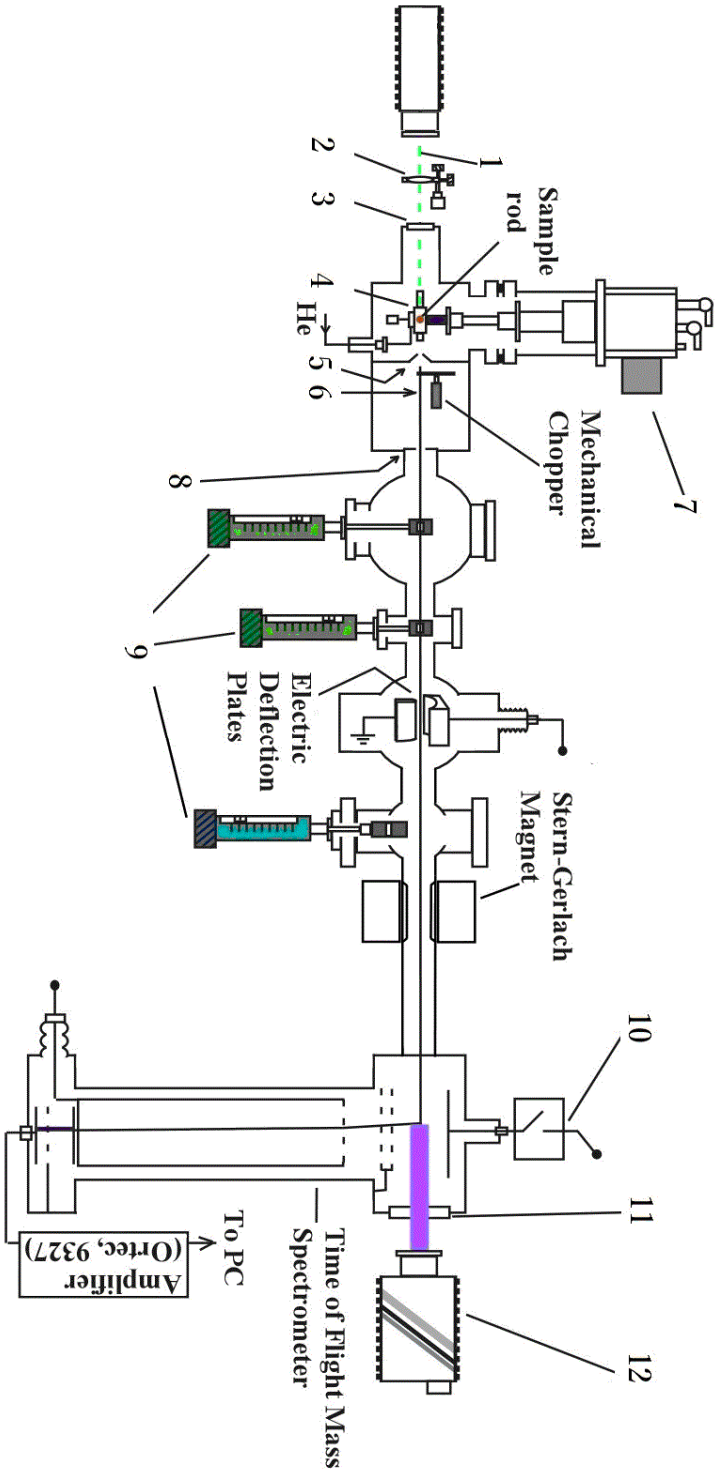
1
2
3
4
He
5
6
7
8
9
10
11
12
Sample rod
Mechanical Chopper
Electric Deflection Plates
Stern-Gerlach Magnet
Time of Flight Mass Spectrometer
To PC
Amplifier (Ortec, 9327)

Figure 1

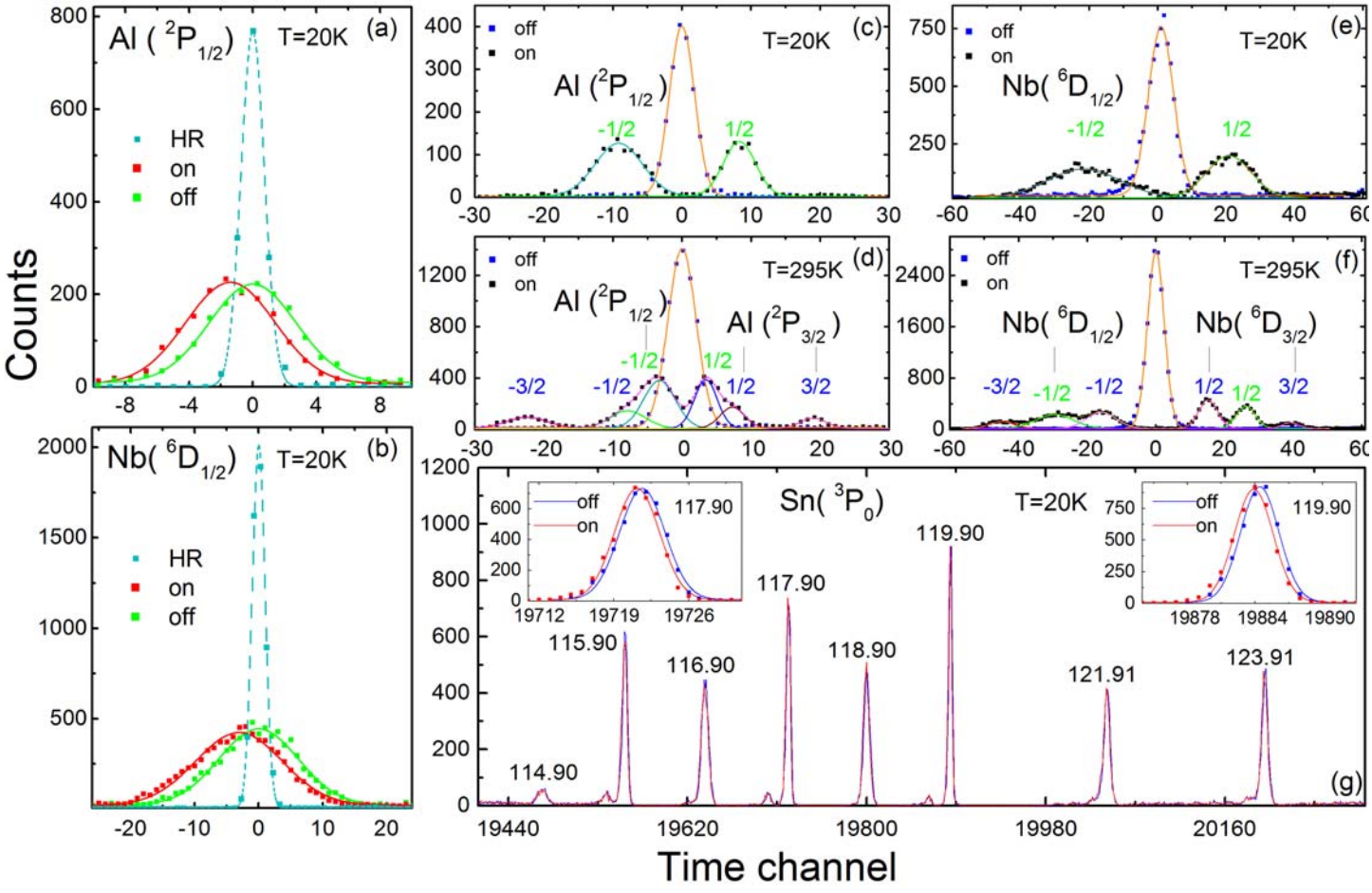
Counts
Time channel
Al ($^2P_{1/2}$) T=20K (a)
HR
on
off
Nb($^6D_{1/2}$) T=20K (b)
off
on
Al ($^2P_{1/2}$) T=20K (c)
-1/2
1/2
Nb($^6D_{1/2}$) T=20K (e)
Al ($^2P_{1/2}$) T=295K (d)
Al ($^2P_{3/2}$)
-3/2
-1/2
1/2
3/2
Nb($^6D_{1/2}$) T=295K (f)
Nb($^6D_{3/2}$)
Sn($^3P_0$) T=20K (g)
114.90
115.90
116.90
117.90
118.90
119.90
121.91
123.91

\

Figure 2

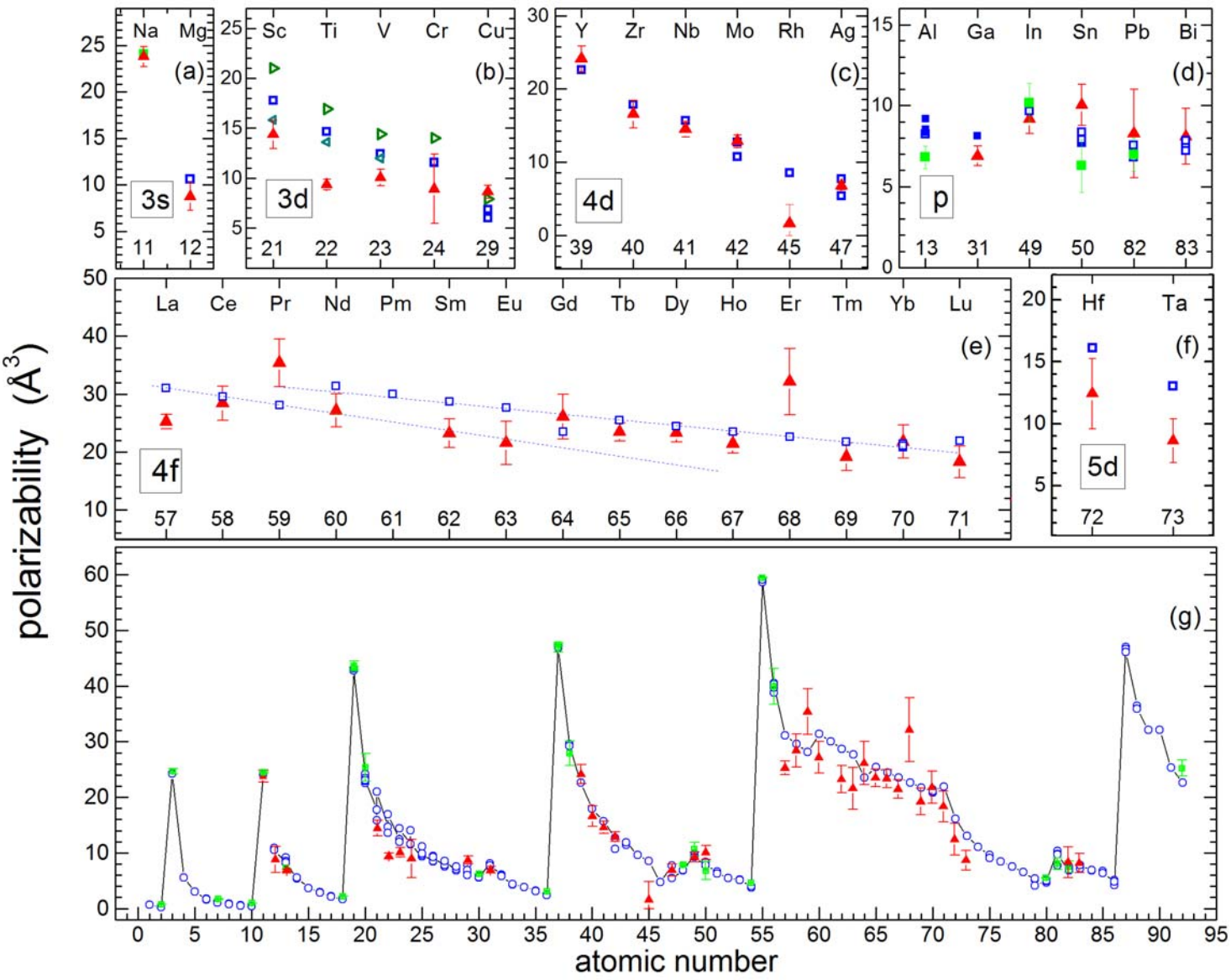
polarizability (Å^3)
Na Mg
(a)
3s
11 12
Sc Ti V Cr Cu
(b)
3d
21 22 23 24 29
Y Zr Nb Mo Rh Ag
(c)
4d
39 40 41 42 45 47
Al Ga In Sn Pb Bi
(d)
p
13 31 49 50 82 83
La Ce Pr Nd Pm Sm Eu Gd Tb Dy Ho Er Tm Yb Lu
(e)
4f
57 58 59 60 61 62 63 64 65 66 67 68 69 70 71
Hf Ta
(f)
5d
72 73
(g)
atomic number

Figure 3

References:

[1] J. W. Schmidt, R. M. Gavioso, E. F. May, and M. R. Moldover, Phys. Rev. Lett. **98**, 254504 (2007)

[2] J. M. Amini and H. Gould, Phys. Rev. Lett. **91**, 153001 (2003)

[3] C. R. Ekstrom, J. Schmiedmayer, M. S. Chapman, T. D. Hammond, and D. E. Pritchard, Phys. Rev. A **51**, 3883 (1995)

[4] G. Maroulis and C. Pouchan, J. Phys. B: At. Mol. Opt. Phys. **36**, 2011, (2003)

[5] J. Mitroy, M. S. Safronova, and C. W. Clark, J. Phys. B: At. Mol. Opt. Phys. **43**, 202001 (2010)

[6] M. T. Murphy, J. K. Webb, and V. V. Flambaum, Phys. Rev. Lett. **99**, 239001 (2007)

[7] T. Rosenband, D. B. Hume, P. O. Schmidt, et al., Science **319**, 1808 (2008)

[8] T. F. Gallagher and W. E. Cooke, Phys. Rev. Lett. **42**, 835 (1979)

[9] W. M. Itano, L. L. Lewis, and D. J. Wineland, Phys. Rev. A **25**, 1233 (1982)

[10] S. G. Porsev and A. Derevianko, Phys. Rev. A **74**, 020502 (2006)

[11] A. D. Ludlow et al., Science **319**, 1805 (2008)

[12] J. A. Sherman, N. D. Lemke, N. Hinkley, M. Pizzocaro, R. W. Fox, A. D. Ludlow, and C. W. Oates, Phys. Rev. Lett. **108**, 153002 (2012)

[13] M. S. Safronova and W. R. Johnson, Adv. At. Mol. Opt. Phys. **55**, 191 (2008)

[14] B. Arora, M. S. Safronova, and C. W. Clark, Phys. Rev. A **76**, 052509 (2007)

[15] A. Derevianko, W. R. Johnson, M. S. Safronova, and J. F. Babb, Phys. Rev. Lett. **82**, 3589 (1999)

[16] A. Hibbert, Rep. Prog. Phys. **38**, 1217 (1975)

[17] V. A. Dzuba, V. V. Flambaum, and M. G. Kozlov, Phys. Rev. A **54**, 3948 (1996)

[18] P. Schwerdtfeger, Table of Experimental and Calculated Static Dipole Polarizabilities for the Electronic Ground States of the Neutral Elements (2014) and references therein, http://ctcp.massey.ac.nz/index.php?menu=dipole&page=dipole

[19] R. W. Molof, H. L. Schwartz, T. M. Miller, and B. Benderson, Phys. Rev. A **10**, 1131 (1974)

[20] H. L. Schwartz, T. M. Miller, and B. Bederson, Phys. Rev. A **10**, 1924 1974

[21] W. F. Holmgren, M. C. Revelle, V. P. A. Lonij, and A. D. Cronin, Phys. Rev. A **81**, 053607 (2010)

[22] NIST, Basic Atomic Spectroscopic Data and references therein, http://physics.nist.gov/PhysRefData/Handbook/periodictable.htm

[23] *CRC Handbook of Chemistry and Physics*, *94th ed.* p10-188 (CRC Press, Boca Raton, FL, 2013-2014) and references therein

[24] P. Milani, I. Moullet, and W. A. de Heer, Phys. Rev. A **42**, 5150 (1990)

[25] G. Scoles, D. Bassi, U. Buck, and D. C. Laine, *Atomic and Molecular Beam Methods*: *Volume 1* (Oxford University Press, Oxford, U.K., 1988)

[26] M. K. Beyer and M. B. Knickelbein, J. Chem. Phys. **126**, 104301 (2007)

[27] C. Thierfelder, B. Assadollahzadeh, P. Schwerdtfeger, S. Schäfer, and R. Schäfer, Phys. Rev. A **78**, 052506 (2008)

[28] S. Schäfer, M. Mehring, R. Schäfer, and P. Schwerdtfeger, Phys. Rev. A **76**, 052515 (2007)

[29] C. Lupinetti and A. J. Thakkar, J. Chem. Phys. **122**, 044301 (2005)

[30] W. A. de Heer and P. Milani, Rev. Sci. Instrum. **62**, 670 (1991)

[31] J. Bowlan, A. Liang, and W. A. de Heer, Phys. Rev. Lett. **106**, 043401 (2011)

[32] R. Moro, X. Xu, S. Yin, and W. A. de Heer, Science **300**, 1265 (2003)

[33] C. Kittel, *Introduction to Solid State Physics, 7th ed.* p412 (John Wiley & Sons, Inc., 1996)

[34] T. P. Guella, T. M. Miller, B. Bederson, J. A. D. Stockdale, and B. Jaduszliwer, Phys. Rev. A **29**, 2977 (1984)